ORIGINAL ARTICLE

A C G publications

Org. Commun. 15:1 (2022) 59-70

organic communications

Structural, spectroscopic, Hirshfeld surface and DFT approach of 3,9-dibromophenanthrene

Osman Çakmak [1,*], C. Cüneyt Ersanlı [2], Kıymet Berkil Akar [3] and Nursel Karaoğlan [4]

[1]*Department of Gastronomy, Faculty of Arts and Design, İstanbul Rumeli University, 34570, İstanbul, Türkiye*
[2]*Department of Physics, Faculty of Arts and Sciences, Sinop University, 57000, Sinop, Türkiye*
[3]*Department of Bioengineering, Faculty of Engineering and Architecture, Tokat Gaziosmanpaşa University, 60150, Tokat, Türkiye*
[44]*Department of Property Protection and Safety Division, TOBB Technical Sciences Vocational School, Karabük University, 78050, Karabük, Türkiye*

(Received November 30, 2021; Revised March 11, 2022; Accepted March 12, 2022)

Abstract: Bromination of 9-bromophenanthrene with one equivalent of bromine resulted in formation of dibromophenantrene isomers. Only 3,9-dibromophenanthrene (**2**) has been isolated from the mixture and characterized by NMR and X-ray diffraction techniques. Solid state crystal structure of dibromide **2** have been established by X-ray diffraction technique. The Hirshfeld and 2D fingerprint analyses were used to investigate the intermolecular interactions in the crystal structure. The molecular geometries have also been optimized by using density functional theory (DFT-B3LYP) methods with the 6-311G (d,p) basis set and geometric parameters have been compared with the experimental data. Additionally, molecular electrostatic potential (MEP), chemical activity parameters, Fukui function (FF) analysis of compound (**2**) have been investigated.

Keywords: Bromophenanthrene; DFT; chemical activity; Hirshfeld surface.

1. Introduction

There are no suitable synthesis methods carried out from the phenanthrene skeletal structure. Thus, phenanthrene derivatives are synthesized using indirect pathways. Most of these have long reaction steps and are not efficient. One of the most common synthesis pathways is the cyclization reactions of stilbenes. This methodology allows the synthesis of a limited number of derivative compounds. For example, 3-bromophenanthrene could be synthesized in 6 reaction steps.[1]

Since bromine can react with many groups in substitution reactions, it makes the structure which it is connected to the key position. Phenanthrene (**1**) is a benzenoid aromatic compound, composed of three-ring. There are 10 different positions to which bromine atoms can be attached. As a result of bromination of phenanthrene (**1**), 25 di-, 61 tri- and 10 tetrabromophenanthrene derivatives can be formed. Due to the difficulty of separation of bromophenanthrenes, bromination reactions of phenanthrene and hence the synthesis of phenanthrene bromides are limited.

* Corresponding author: E-Mail: cakmak.osaman@gmail.com, Phone: + 90 2128660101; Fax: + 90 2128660125.

The article was published by ACG Publications
http://www.acgpubs.org/journal/organic-communications © January-March 2022 EISSN:1307-6175
DOI: http://doi.org/10.25135/acg.oc.119.2109.2213
Available online: March 16, 2022

Since the isomeric multiplicity, studies aimed at increasing the selectivity in the production of bromophenanthrenes come into prominence and gain importance. So far, there has been no significant development in this field.

In our group studies, it was shown that aromatic compounds can be brominated by using less solvent as well as prolonging reaction time without using Lewis acid catalysts such as iron in bromination reactions. The longer the reaction time, the greater the selectivity. At the same time, temperature, the use of different solvents, and the use of support catalyst increase selectivity. Likewise, the amount of bromine and the radicalic conditions in the presence of light, change the selectivity, yield and reactivity in the reactions. Likewise, the amount of bromine and the radicalic conditions in the presence of light change the selectivity, yield and reactivity in the reactions.[2-4]

This study constitutes the first result of the tentative study. X-ray analysis of the products formed over a long reaction time and separated by crystallization was reported.

The title compound of 3,9-dibromophenanthrene (**2**) has been synthesized and characterized mainly by X-ray diffraction technique in this work. While the structural and electronic properties of the title molecule are determined experimentally by spectroscopic techniques (FTIR, ^{1}H NMR, ^{13}C NMR) and all theoretical analysis are calculated by DFT-B3LYP/6-311G (d,p) method. Hirshfeld surface (HF) analysis was used to analyze the inter-molecular interactions in the crystal structures. Besides these, MEP maps, chemical activity parameters, net charges, FF analysis are discussed and revealed the nucleophilic and electrophilic nature of (**2**). Polarizability (α) and the first hyperpolarizability (β) were calculated to investigate the effect of the π-electron system and exhibition NLO active material. NLO materials have gained attention for their future potential applications in the field of optoelectronic such as optical switching processing, optical computing and optical communication. A complete description of molecular and chemical activity (electrophilic and nucleophilic structure) was given to the titled paper, which includes experimental and theoretical studies.

2. Experimental

2.2. Chemistry

2.2.1. Synthesis of 9-Bromophenantrene

In this experiment, the starting compound 9-bromophenanthrene (**1**) was prepared for future studies. High-efficiency reaction conditions for 9-bromphenanthrene were determined by addition-displacement reactions. 9-bromophenantrene was synthesized based on the method described by Dornfeld *et al*.[5] with some modifications on the reaction vessel. A two-necked reaction flask was equipped with a condenser (drying tube) and a dropping funnel on each neck. To a boiling solution of phenanthrene (20 g, 0.112 mol) in 30 mL CCl_4 was added drop-by-drop (using the dropping funnel) a solution of 5.8 mL bromine (18.076 g, 0.113 mol, 1 eq) in 5 mL CCl_4 over an hour. The mixture was stirred using a magnetic stirrer and boiled under reflux for 9 hours. The reaction process was monitored by thin layer chromatography. Later phenanthrene (**1**) completely reacted, the reaction content was filtered through flash SiO_2 column (20 g) using hexane (28.76 g) as the mobile phase. 9-Bromphenanthrene (**2**) was crystallized in a refrigerator using low amount of CH_2Cl_2-pentane solvent system. 9-bromophenanthrene (**2**) (25.92 g) was obtained in 90% yield.

2.3. X-ray Crystallography

The X-ray diffraction data for (**2**) was collected using a Bruker Smart CCD diffractometer. The X-ray source was MoKα (λ = 0.71073 Å). APEX-II[8] and Bruker SAINT [8] software were used during collecting data and refining cell, respectively. We also used ORTEP III[9] and WinGX software[10]programs to construct figures. The programs used for solving and refining the molecular structure were SHELXS-97 [11]and SHELXL-97[11], respectively. The ring puckering parameters were calculated used PLATON. [12]All non-hydrogen atom parameters were refined anisotropically and all hydrogen atoms were located in their idealized positions and refined using a riding model. Conditions for data collection and parameters of the refinement process are listed in Table 1.

2.4. Computational Procedures

All calculations were performed by using Gaussian03W[13] program package at the DFT level of theory by using the hybrid functional B3LYP (Becke's three-parameter hybrid functional using the LYP correlation functional)[14, 15] with 6-311G (d,p) basis set. Their results were visualized using the GaussView molecular visualization program[16]. HS analysis was used to explore the molecular interactions by using the Crystal Explorer program. [17]

3. Results and Discussion

3.1. Chemistry

There are very few studies on the synthesis of 3,9-dibromophenanthrene (**2**). Previously, the synthesis of the 3,9-dibromophenanthrene (**2**) *via* bromination of phenanthrene has been reported by Henstock.[6] Bromination of phenanthrene using 2 or 3 mole equivalents of molecular bromine in carbon tetrachloride at 30 °C gave a mixture of 9-bromophenanthrene (**1**) and 3,9-dibromophenanthrene (**2**) in low yields, and there is no adequate experimental and spectroscopic data.[6] In an another work, 3,9-dibromophenanthrene (**2**) was synthesized by Schwechten's modification of the Sandmeyer reaction of diazonium salt, which is obtained *via* diazotized of 3-amino-9-bromophenanthrene (yield: 57%) (**5**).[7]

In this study, the bromination of 9-bromophenanthrene (**1**) at -18 °C with one equivalent of bromine in dichloromethane afforded a mixture of three dibromophenanthrenes (3,9-dibromophenanthrene **2**, 1,9-dibromophenanthrene **3** and 9,10-dibromophenanthrene **4**). Subsequent crystallization from dichloromethane/hexane gave pure 3,9-dibromopehananthrene (**2**) (13%) (Scheme 1). Only dibromide 2 was purely isolated. Other isomers were established proton NMR analysis of the mixture.

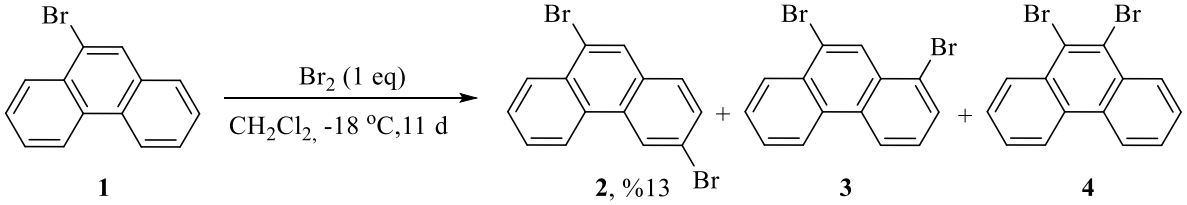

Scheme 1. Synthesis of the 3,9-dibromophenanthrene (**2**)

*3.2. Crystal Structure of (**2**)*

Atom numbering scheme of (**2**) is shown in Fig. 1 and selected geometric parameters are given in Table 2. The compound (**2**) is crystallized in the monoclinic space group *P21/c*. In the title compound (Fig. 1), there is a weak intra-molecular C2–H2···Br1 hydrogen bond (Table 3).

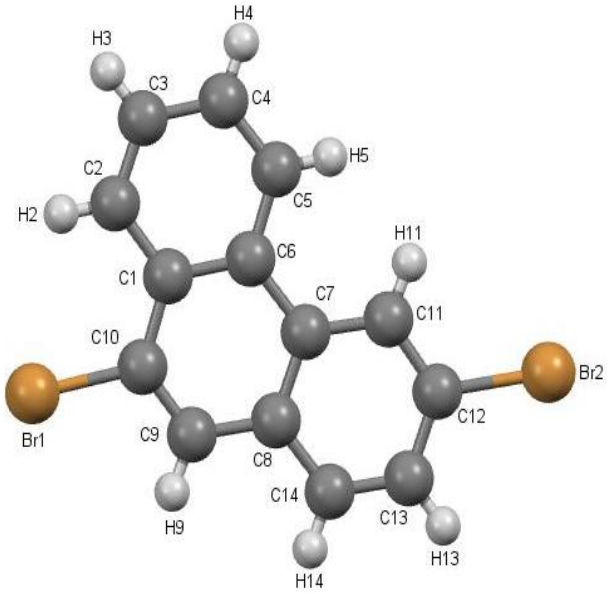

Figure 1. The molecular structure of (**2**).

Table 1. Crystal data and structure refinement parameters for (**2**)

	2
Chemical formula	$C_{14}H_8Br_2$
Formula weight	336.02
Temperature (K)	296
Crystal system	Monoclinic
Space group	P 21/c
Unit cell parameters (Å, °)	
a	3.9624(11)
b	24.445(7)
c	11.825(4)
α	90
β	93.722(10)
γ	90
Volume ($Å^3$)	1143.0(6)
Z	4
Density (g/cm^3)	1.953
Absorption coefficient (mm^{-1})	7.057
T_{min}, T_{max}	0.5735, 0.7454
θ range for data collection	3.04° to 26.78°
Unique reflections measured	24378
Independent/observed reflections	2286/1618
Data/restraints/parameters	2420/0/146
Goodness of fit on F^2	1.161
R [$I>2\sigma(I)$], *wR*	0.061/0.127
CCDC number	2122692

The dihedral angles between the Cg1(C1-C6) and Cg2(C1/C6-C10), Cg2(C1/C6-C10) and Cg3 (C7/C8/C11-C14), Cg1(C1-C6) and Cg3(C7/C8/C11-C14) rings are 0.417(4)°, 0.624(4)° and 0.899(4)°. Therefore, the title compound can be proposed to has a planar molecular structure. The largest deviations from the best planes are 0.0063(7)Å for C3, 0.0030 (6) Å for C10 and 0.0094(6) Å for C12. The halogen···halogen contacts (C–X1···X2–C) are generally classified as Type I and Type II based on the distances (X1···X2) and angles (θ1=C–X1···X2 and θ2=X1···X2–C) between halogens. There are two different ways of Type I interaction, which correspond to the arrangement of atoms in *trans* and *cis*

geometries. On the other hand, Type II interaction is defined by a single geometry in which the atoms are lined up to form an *L*-shape. θ1 and θ2 angles are equal or close to each other in Type I while they are approximately 180° and 90° in Type II[20]. The crystallographic studies show the presence of C-Br···Br-C interactions in the title compound as seen Fig. 2. The Br1···Br1 distance is 5.057(4) Å, and θ1 and θ2 angles are 162.38(4)° and 163.04(4)°, respectively. Based on these values, the intermolecular C12^{i}-Br2^{i}···Br1-C10 (i: *-x*, ½+*y*, ½-*z*) and C12-Br2···Br1^{ii}-C10^{ii} (ii: *x*, *y*, *1*+*z*) interactions can be best described as a Type I interaction (θ1 and θ2 angles are nearly equal). In addition, the crystal structure is stabilized via π···π interactions. In the title molecule, Cg1···Cg1^{i} [3.963(5) Å], Cg1···Cg1^{ii} [3.962(5) Å], Cg2···Cg2^{i} [3.963(4) Å], Cg2···Cg2^{ii} [3.962(4) Å], Cg3···Cg3^{i} [3.962(5) Å] and Cg3···Cg3^{ii} [3.963(5) Å] interactions are also effective in crystal packing [(i):*-1*+*x*,*y*,*z*; (ii): *1*+*x*,*y*,*z*]. The packing diagram of the compound (**2**) is illustrated in Fig. 2.

Table 2. Bond lengths (Å), bond and torsion angles (°) were obtained by X-ray (experimental) and DFT/B3LYP/6-311G(d,p)

Bond lengths (Å), Bond and Torsion angles (°)	Experimental	DFT
C1-C6	1.426(9)	1.4257
Br1-C10	1.913(7)	1.9122
Br2-C12	1.909(7)	1.9089
C7-C11	1.417(9)	1.4175
C11-C12	1.377(9)	1.3771
C7-C8	1.377(9)	1.4286
C9-C10	1.330(10)	1.3311
C1-C10-Br1	117.5(5)	119.447
C11-C12-Br2	118.8(5)	118.8291
C6-C7-C11	122.9(6)	122.8948
C2-C1-C10	123.3(6)	123.297
C2-C1-C10-Br1	0.2(10)	0.1157
C14-C13-C12-Br2	179.0(6)	179.1214
C5-C6-C7-C11	1.1(11)	1.1376
C1-C10-C9-C8	0.5(11)	0.5945

The theoretical and experimental bond length and angle values of the title molecule are given in Table 2. Due to neglecting all non-solid interactions in the theoretical calculations, some differences were observed between the experimental and calculated parameters in Table 2. These differences are not surprising as the calculations are carried out on a single molecule isolated in the gaseous-phase.

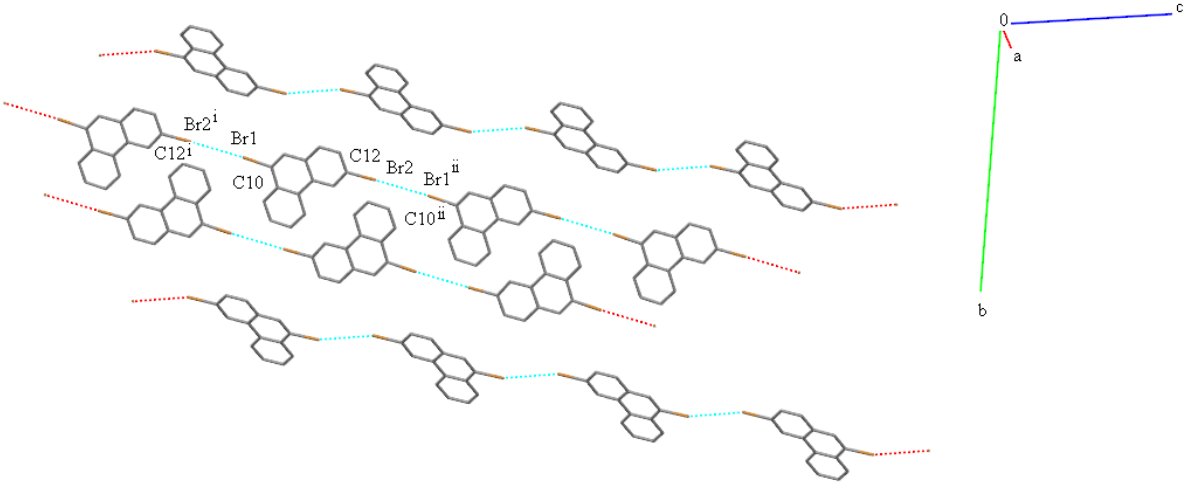

Figure 2. The C-Br···Br-C interactions in title compound

Table 3. Hydrogen bonding and short contact geometries (Å, °) for (**2**)

D–H···A	D–H	H···A	D···A	D–H···A
C2–H2···Br1	0.93	2.76	3.194(8)	110

D: Donor; A: Acceptor

3.3. Hirshfeld Surface (HS) Analysis

HS analysis surveys the intermolecular interactions in terms of surface contribution and generating graphical representations, plotting 2D fingerprint plots, [21, 22] and generating electrostatic potential. [23] The electrostatic potential surfaces are figured with the red region for is a negative electrostatic potential (hydrogen acceptors) and blue region for a positive electrostatic potential (hydrogen donor).

The distance from the surface to the nearest inner surface of the atom is known as d_i, while d_e represents the distance from the surface to the nearest outer surface of the atom[24]. Gray is the outline of the full fingerprint, and blue refers to the low occurrence frequency of the (d_i, d_e) pair. The d_{norm} (normalized contact distance) values are mapped onto the HS by using three different colors (red–blue–white), where red spots show the shortest contacts, blue shows longer contacts and white spots are assigned to the contacts that are around the van der Waals separation. The d_{norm}, d_i, d_e, shape and curvedness indexes are -0.0335 to 1.0408, 1.1436 to 2.4576, 1.1450 to 2.6844, -1 to 1 and -4 to 4 Å for (Fig. 3). In the form of a shape index, adjacent red and/or blue triangles describe the π**…**π interactions. So, in the title molecule, the shape index figure suggests that there are π**…**π interactions. The crystal packing diagrams on d_{norm} surface is shown in Fig. 4. Reciprocal Br**…**H 30.5%, Br**…**H 30.1%, C**…**C 15.6%, Br**…**C 4.1% and C**…**H 14.6% inter-molecular interactions are the most abundant (Fig. 5).

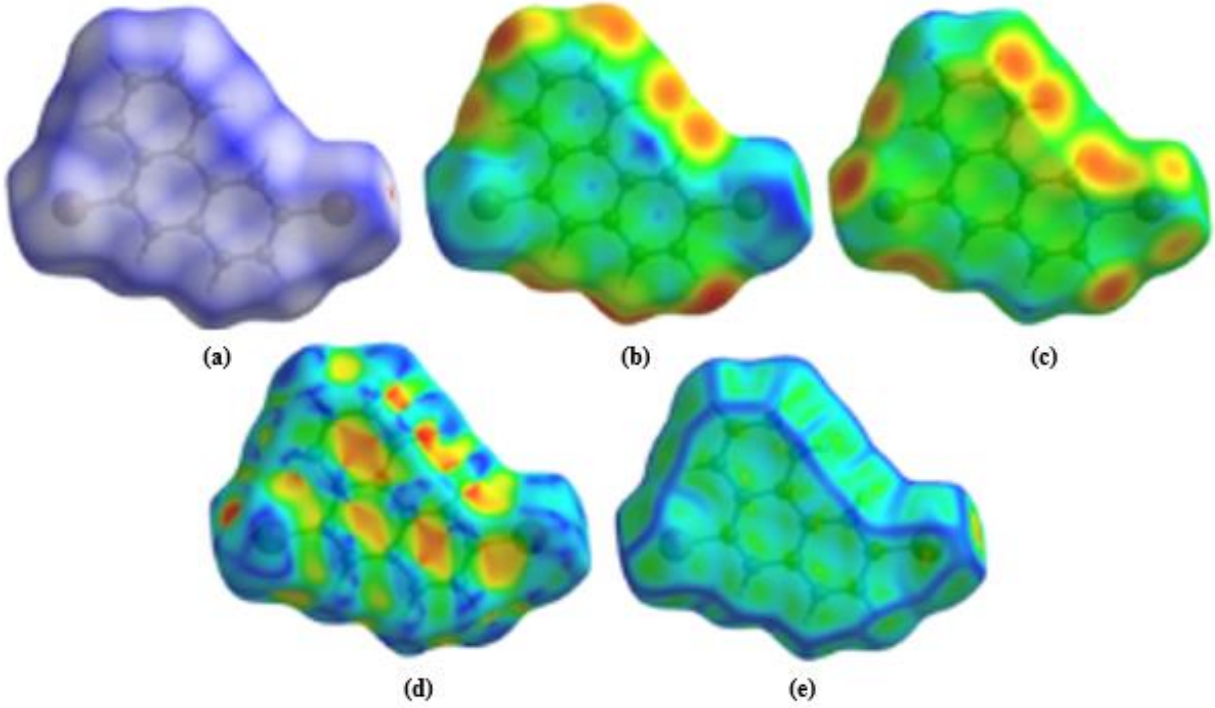

Figure 3. Hirshfeld surfaces of (**2**)

Figure 4. HS mapped with d_{norm} shows C-Br···Br-C interactions

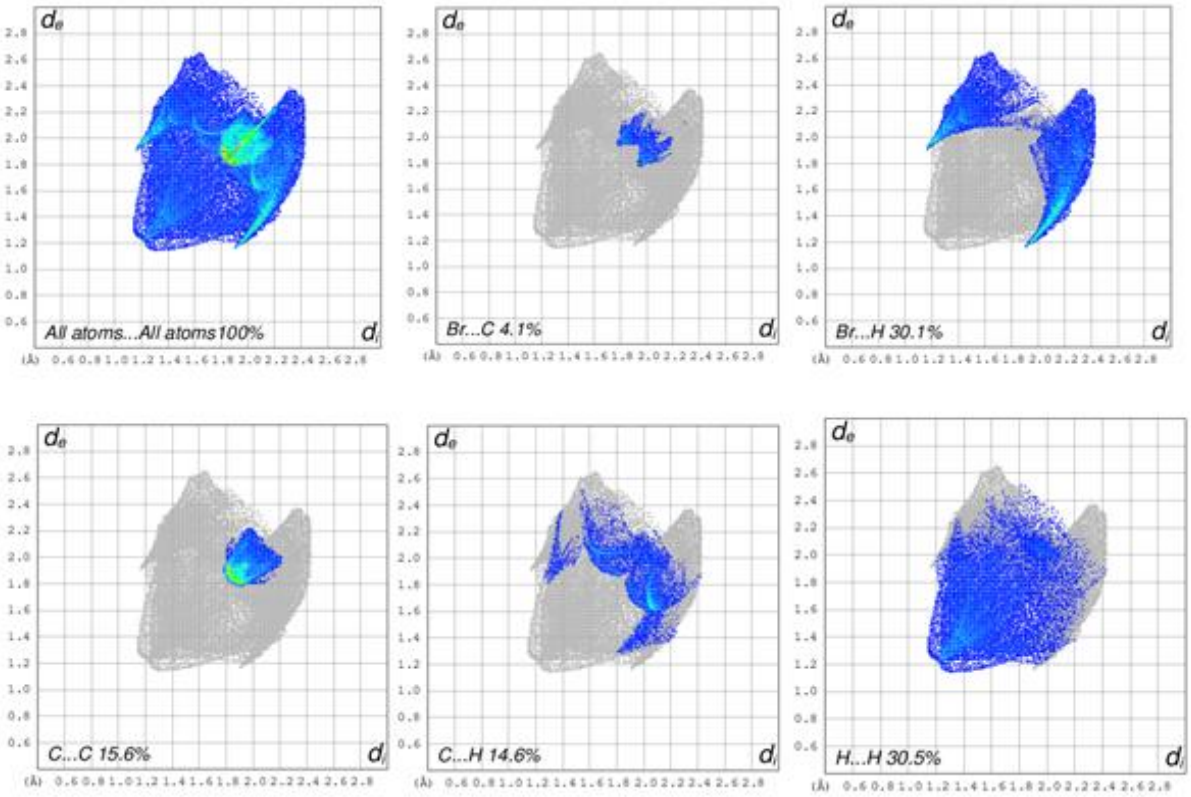

Figure 5. Fingerprint plots of (**2**)

3.4. Frontier Molecular Orbitals (FMOs) and Chemical Activity Parameters

The frontier orbital gap helps in characterizing the chemical reactivity and determine the intramolecular charge transfer. The HOMO symbolizes electron donating ability, while the LUMO represents electron accepting ability. As both the HOMO and LUMO orbitals supports to describe the chemical reactivity and kinetic stability of molecule. The energy gap of HOMO–LUMO helps to explains the charge transfer interaction within the molecule. The energy difference of energy gap (ΔE) qualifies the molecular chemical stability of the molecules[25, 26]. The FMOs computed and the relevant figures are given in Fig. 6.

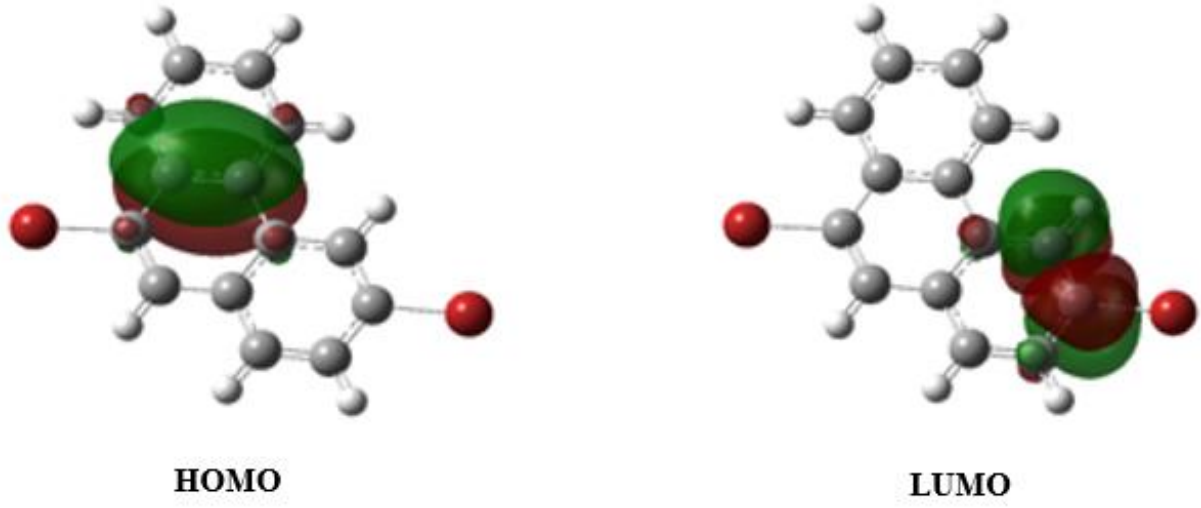

Figure 6. HOMO and LUMO orbitals of (**2**)

The chemical reactivity descriptors associated with title molecule is calculated as follows: ionization potential I = 6.92 eV, electron affinity A = 0.28 eV, electronegativity χ= (I +A)/2 = 3.6 eV, global hardness η =(I-A)/2 =3.32 eV, softness (S=1/2 η) = 0.150 eV^{-1}, chemical potential μ= -(I + A)/2 = -3.6 eV and electrophilicity index $w=\mu^2/2\,\eta$ = 1.95 eV.

The title molecule shows a large energy gap, lower value of softness and higher value of hardness. The title compound (**2**) is hard because the ΔE=6.64 eV is very large and it is usually connected with a lower chemical reactivity and high kinetic stability. Also, according to chemical reactivity descriptors results, low softness [0.15 $(eV)^{-1}$] and high hardness (3.32 eV) parameters display that the title compound (**2**) has high kinetic stability, lower chemical reactivity and lower intramolecular charge transfer.

3.5. Molecular Electrostatic Potential (MEP)

The MEP is used as a reactivity map for understanding sites of nucleophilic (positive potential) and electrophilic (negative potential) reactions[27, 28]. Molecular electrostatic potential (MEP) mapping explains the nucleophilic and electrophilic regions in compounds. The chemical behavior of a system predicts an electrophilic and nucleophilic site on the basis of color code in a molecule. MEP is a basic property, which explains the behavior of purpose molecule and demonstrates the relative polarity of a compound. As can be seen from the MEP of the title molecules, while regions having the negative potential are over the bromine atoms, the regions having the positive potential are over the hydrogen atoms (Fig. 7). The MEP contour plot is related to relative electron density. According to Fig. 10, there are yellow or red zones around the nitrogen and bromine atoms of investigated molecules in MEP maps. The contour maps are used to show lines of constant density or brightness, such as electrostatic potentials respect drawn in the molecular plane. The electron-rich redlines are around bromine atoms whereas electron-deficient regions are shown by greenish-yellow lines for a mentioned molecule.

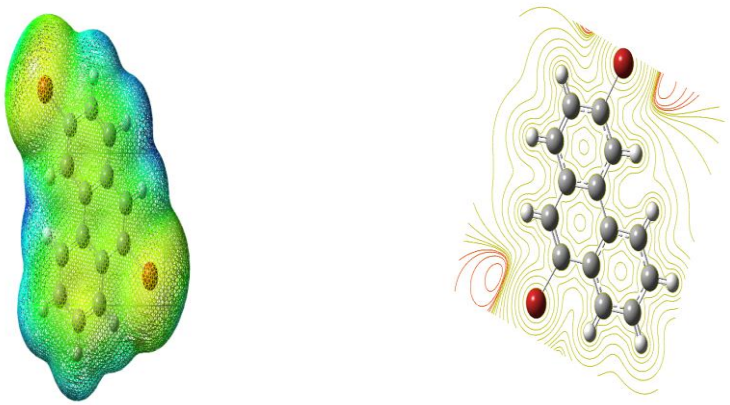

MEP **MEP CONTOUR**

Figure 7. MEP and MEP contour of title compound (**2**)

3.6. Net Charges of Mulliken Population (MP) and Fukui Function (FF) Analyses

The calculation of atomic charges (Mulliken population analysis) describes the electronic characteristics of molecular systems. The charge distribution on the molecule is helpful to describe the processes of electronegativity equalization and charge transfer in chemical reactions also to model of the electrostatic potential outside molecular surfaces. The Mulliken atomic charges derived from Mulliken population analysis directly and ensures a means of estimating partial atomic charges[29, 30]. According to MP result, the most negative atomic charges are show C12>C10>C8>C6>C4>C3>C7>C14>Br1>Br2>C2>C5 atoms (electrophilic attack). Also, the most positive atomic charges (C9>C11>C13>C1) are positioned on all hydrogen atoms (Table 4). We calculated the reactive behavior of the studied molecule electrophilic and nucleophilic reactions by net charge analysis.

Table 4. Mulliken population charges of optimized structure (**2**)

Atoms	MP Charges	Atoms	MP Charges
C1	0.020986	C9	0.102109
C2	-0.029267	C10	-0.217242
C3	-0.063185	C11	0.090978
C4	-0.072442	C12	-0.240928
C5	-0.021601	C13	0.042196
C6	-0.077188	C14	-0.049534
C7	-0.060674	Br1	-0.037916
C8	-0.079671	Br2	-0.031670

The FF gives information about local site reactivity on the entire molecule and is one of the most widely used among local reactivity determinants. The position prone to nucleophilic, electrophilic and radical attack in the title compound has been assessed using the FF. The more practical and convenient way to access the FF at an atomic level is to use the condensed FFs[31] which are expressed as $f_k^+(r)$ for nucleophilic attack(r), $f_k^-(r)$ for electrophilic attack (r) and $f_k^0(r)$ for free radical attack (r). As could be seen in Table 5, the atoms of C2, C3, C5, C7 and C8 ($\Delta f_k(r)$>0) are tend to nucleophilic attack whereas C1, C4, C6, C9, C10, C11, C12, C13, C14, Br1 and Br2 ($\Delta f_k(r) <$ 0) atoms indicate the electrophilic attack.

Table 5. Values of the FF considering natural population analysis for (**2**).

Atom	q^0_k	q_k^+	q_k^-	f_k^-	f_k^+
C1	-0.08795	-0.10290	-0.08369	-0.00426	-0.01495
C2	-0.17509	-0.10580	-0.23781	0.06272	0.06929
C3	-0.18501	-0.16813	-0.19913	0.01412	0.01688
C4	-0.18376	-0.11229	-0.27373	0.08997	0.07147
C5	-0.17498	-0.13571	-0.19659	0.02161	0.03927
C6	-0.02036	-0.01608	-0.05226	0.0319	0.00428
C7	-0.01821	0.01326	-0.03739	0.01918	0.03081
C8	-0.04638	-0.02847	-0.04442	-0.01938	0.01791
C9	-0.20772	-0.13693	-0.32113	0.11341	0.07079
C10	-0.04374	0.02268	-0.11901	0.07527	0.06642
C11	-0.21138	-0.18680	-0.25756	0.04618	0.02458
C12	-0.06956	-0.01303	-0.13392	0.06436	0.05653
C13	-0.17498	-0.21232	-0.23336	0.07348	-0.03734
C14	-0.15670	-0.10259	-0.23018	0.07348	0.05411
Br1	0.05281	0.21035	-0.10719	0.16000	0.15754
Br2	0.05555	0.21563	0.22787	0.17232	0.16008

3.7. Nonlinear Optical (NLO) Effects

NLO is at the forefront of current research due to its importance in providing key functions of frequency shifting, switching, optical modulation, fiber, laser, optical materials logic and optical memory for the emerging technologies in areas such as optical interconnections, telecommunications and signal processing[30, 32]. It is well known that the higher values of dipole moment, molecular polarizability, and hyperpolarizability are important for more active NLO properties. HOMO and LUMO molecular orbitals play a key role in NLO properties of the molecule[33]. If the HOMO-LUMO energy range of a molecule is small, it is relatively possible for electrons to move from HOMO to LUMO. This mobility in the electronic arrangement will increase the polarity hence the NLO properties.

Urea (β value is $0.13x10^{-30}$ cm^5/esu) obtained by B3LYP/6-311 G(d,p) method is one of the reference materials to compare NLO properties of a conjugated organic compound[34]. The calculated values of dipole moment (μ), polarizability (α) and the first hyperpolarizability (β) are 2.51 D, 29.46 $Å^3$ and $1.67x10^{-30}$ cm^5/esu. When it is compared to urea, the calculated value of β of the compound (**2)** is approximately 12.8 times that of urea making it an effective candidate for NLO studies in the future.

3.8. Vibrational Spectra

Vibrational spectroscopy is widely used in organic chemistry for the identification of functional groups of organic compounds with the help of fundamental modes observed and calculated. The calculated frequencies were slightly different from the experimental values for the normal modes. The reason for these small differences is perhaps in the experimental process in which we recorded spectra with a solid-phase sample, but the DFT calculations were made with an isolated and gaseous-phase molecule.

The aromatic C–C stretching modes occur in the region 1650-1430 cm^{-1} [35]. These modes were observed at 1580 cm^{-1} (experimentally) and 1540-1567 cm^{-1} (theoretical). In literature, C–H stretching modes of the benzene rings occur above 3000 cm^{-1} [36]**.** The aromatic C–H symmetric stretching modes were calculated at 3102 cm^{-1} and asymmetric ones are in the range of 3066-3092 cm^{-1} as theoretically. The same bands were observed just to the left of 3000 cm^{-1} in the experimental spectrum. Also, there is a band at 890 and 910 cm^{-1} for Br-C stretching vibrations in theoretical and experimental FTIR spectrum, respectively. Some of the characteristic frequencies were illustrated in Table 6 as comparatively.

Table 6. Some characteristic IR absorption bands for (**2**).

Compound	**(2)**	**Compound**
Assignments	**Experimental (cm^{-1})**	**Assignments**
C–H *(symm) str.*	3100	3102
C–H *(asymm) str.*	3100	3092
C-C *str.*	1580	1540-1567
Br–C *str.*	910	890
C–H (arom.) *bend.*	1100-1500	1244-1462

str. : stretching, bend. : bending, arom. : aromatic

4. Conclusion

The title compound of 3,9-dibromophenanthrene (**2**) has been synthesized and characterized by FTIR and NMR spectroscopic techniques. Solid state crystal structure of (**2**) has been determined by a single-crystal X-ray diffraction technique. The crystal structure is stabilized by C-Br···Br-C interactions and they can be best described as a Type I interaction (θ1 and θ2 angles are nearly equal). HS analysis is used to visualize the fidelity of the crystal structure. All theoretical calculations were carried out by using DFT-B3LYP/6-311G (d,p) method. The theoretical geometric parameters were found to be in good agreement with X-ray diffraction results. The electrophilic and nucleophilic reactivity is determined by MEP and net charge analysis results. The higher value of HOMO-LUMO energy gap of the compound (**2**) shows the good stability and high chemical hardness of the studied compound. The title molecule has lower intra-molecular charge transfer, higher kinetic stability and lower chemical reactivity. Also, the title compound (**2)** is approximately 12.8 times that of urea making it an effective candidate for NLO studies in the future. We hope the results of this study will help researchers in the design and synthesis of new phenanthrene compounds.

Acknowledgements

The author acknowledges Scientific and Technological Research Application and Research Center (SUBITAM), Sinop University, Turkey, for the use of the Bruker D8-QUEST diffractometer.

Supporting Information

Supporting information accompanies this paper on http://www.acgpubs.org/journal/organic-communications

ORCID
Osman Çakmak: 0000-0001-9293-5572
C. Cüneyt Ersanlı: 0000-0002-8113-5091
Kıymet Berkil Akar: 0000-0001-9993-9541
Nursel Karaoğlan: 0000-0002-1641-9258

References

[1] Ogawa, Y.; Ueno, T.; Karikomi, M.; Seki, K.; Haga, K.; Uyehara, T. Synthesis of 2-acetoxy[5]helicene by sequential double aromatic oxy-Cope rearrangement. *Tetrahedron* **2002**, *43*, 7827-7829.
[2] Çakmak, O.; Aydoğan, L.; Berkil, K.; Gülçin, İ.; Büyükgüngör, O. Highly brominated anthracenes as precursors for the convenient synthesis of 2,9,10-trisubstituted anthracene derivatives. *Beilstein J. Org. Chem.* **2008**, *4*, 50.
[3] Çakmak, O.; Demirtaş, I.; Balaydın, H.T. Selective bromination of 1-bromonaphthalene: efficient synthesis of bromonaphthalene derivatives. *Tetrahedron* **2002**, *58*, 5603-5609.
[4] Tutar, A.; Çakmak, O.; Karakaş, M.; Önal, A.;İde, S. Highly brominated biphenylenes as precursors for the convenient synthesis of 5,6,8,10-tetrabromobenzocyclooctene. *J. Chem. Res.* **2004**, *8*, 545-549.
[5] Dornfeld, C.A.; Callen, J.E.; Coleman, G.H. 9-Bromophenanthrene. *Org. Synth.* **1955**, *3*, 134.
[6] Henstock, H. CCCLXV.-The bromine compounds of pheranthrene. Part II. *J. Chem. Soc., Trans.* **1923**, *123*, 3097-3099.
[7] Schultz, J.; Goldberg, M.A.; Ordas, E.P.; Carsch, G. Attempts to find new antimalarials. IX. Derivatives of phenanthrene, I. Amino alcohols of the type -CHOHCH2NH2, derived from 9-bromophenanthrene. *J. Org. Chem*. **1946**, *11*, 307-313.
[8] Bruker APEX-II, SAINT and SADABS. Bruker AXS Inc., Madison, Wisconsin, USA, 2013.
[9] Farrugia, L.J. ORTEP-III for Windows- a version of ORTEP-III with a Graphical User Interface (GUI). *J. Appl. Crystallogr*. **1997**, *30*, 565.
[10] Farrugia, L.J. WinGX suiteforsmall-moleculesingle-crystalcrystallography. *J. Appl. Crystallogr*. **1999**, *32*, 837-838.
[11] Sheldrick, G.M. SHELXS97 and SHELXL97, University of Göttingen, Germany, **1997**.
[12] Spek, A.L. PLATON, Utrecht University, The Nethetlands, **2000**.
[13] Frisch, M.J.; Trucks, G.W.; Schlegel, H.B.; Scusseria, G.E.; Robb, M.A.; Cheeseman, J.R.; Montgomery, J.A.; VrevenJr., T.; Kudin, K.N.; Burant, J.C.; Millam, J.M.; Iyengar, S.S.; Tomasi, J.; Barone, V.; Mennucci, B.; Cossi, M.; Scalmani, G.; Rega, N.; Petersson, G.A.; Nakatsuji, H.; Hada, M.; Ehara, M.; Toyota, K.; Fukuda, R.; Hasegawa, J.; Ishida, M.; Nakajima, T.; Honda, Y.; Kitao, O.; Nakai, H.; Klene, M.; Li, X.; Knox, J.E.; Hratchian, H.P.; Cross, J.B.; Adamo, C.; Jaramillo, J.; Gomperts, R.; Stratmann, R.E.; Yazyev, O.; Austin, A.J.; Cammi, R.; Pomelli, C.; Ochterski, J.W.; Ayala, P.Y.; Morokuma, K.; Voth, G.A.; Salvador, P.; Dannenberg, J.J.; Zakrzewski, V.G.; Dapprich, S.; Daniels, A.D.; Strain, M.C.; Farkas, O.; Malick, D.K.; Rabuck, A.D.; Raghavachari, K.; Foresman, J.B.; Ortiz, J.V.; Cui, Q.; Baboul, A.G.; Clifford, S.; Cioslowski, J.; Stefanow, B.B.; Liu, G.; Liashenko, A.; Piskorz, P.; Komaromi, I.; Martin, R.L.; Fox, D.J.; Keith, T.; Al-Laham, M.A.; Peng, C.Y.; Nanayakkara, A.; Challacombe, M.; Gill, P.M.W.; Johnson, B.; Chen, W.; Wong, M.W.; Gonzalez, C.; Pople, J.A. Gaussian IncWallingfırd, CT, **2004**.
[14] Becke, A.D. Density-functional exchange-energy approximation with correct asymptotic behavior. *Phys. Rev*. **1988**, *38*, 3098-3100.
[15] Lee, C.; Yang, W.; Parr, R.G. Development of the Colle-Salvetti correlation-energy formula into a functional of the electron density. *Phys. Rev. B Condens. Matter*. **1988**, *37*, 785-789.
[16] Dennington, R.; Keith, T.; Millam, J.; GaussView, Version 4.1.2, Semichem, Inc., Shawnee Mission, KS, **2007**.
[17] Turner, M.J.; McKinnon, J.J.; Wolff, S.K.; Grimwood, D.J.; Spackman, P.R.; Jayatilaka, D.; Spackman, M.A. Crystal Explorer 17, The University of Western Australia, Perth, Australia, **2017**.
[18] Manso, M.; Fenandez, L.; Wang, Z.İ.; Moth-Poulsen, K.; Brondsted Nielsen, M. Donor-Acceptor Substituted Benzo-, Naphtho- and Phenanthro-Fused Norbornadienes. *Molecules* **2020**, *25*, 322.

[19] Nesmeyanov, A.N.; Tolstaya, T.P.; Vanchikova, L.N.; Petrakov, A.V. Oxidative cyclization of α-(o-iodophenyl)cinnamic acids as a new route to certain phenanthrene derivatives. *Bull. Acad. Sci. USSR*. **1980**, *29*, 1789-1792
[20] Hathwar, V.R.; Roopan, S.M.; Subashini, R.; Khan, F.N.; Row, T.N.G. Analysis of Cl… Cl and CH…Cl intermolecular interactions involving chlorine in substituted 2-chloroquinoline derivatives. *J. Chem. Sci.* **2010**, *122*, 677-685.
[21] Gümüş, M.K.; Kansız, S.; Aydemir E.;Gorobets, N.Y.; Dege, N. Structural features of 7-methoxy-5-methyl-2-(pyridin-3-yl)-11,12-dihydro-5,11-methano[1,2,4]triazolo[1,5-*c*] [1,3,5]benzoxadiazocine: Experimental and theoretical (HF and DFT) studies, surface properties (MEP, Hirshfeld). *J. Mol. Struct.* **2018**, *1168*, 280-290.
[22] Seth, S.K.Tuning the formation of MOFs by pH influence: X-ray structural variations and Hirshfeld surface analyses of 2-amino-5-nitropyridine with cadmium chloride. *Cryst. Eng. Commun.* **2013**, *15*, 1772-1781.
[23] Seth, S.K. Structural elucidation and contribution of intermolecular interactions in *O*-hydroxy acyl aromatics: Insights from X-ray and Hirshfeld surface analysis. *J. Mol. Struct.* **2014**, *1064*, 70-75.
[24] Parkin, A.; Barr, G.; Dong, W.; Gilmore, C.J.; Jayatilaka, D.; McKinnon, J.J.; Spackman, M.A.; Wilson, C.C. Comparing entire crystal structures: structural genetic fingerprinting. *Cryst. Eng. Commun.* **2007**, *9*, 648-652.
[25] Demircioğlu, Z.; Ersanlı, C.C.; Kaya Kantar, G.; Saşmaz, S. Spectroscopic, Hirshfeld surface, X-ray diffraction methodologies and local & global chemical activity calculations of 5-(2-methoxy-4-(prop-1-en-1-yl)phenoxy)pyrazine-2,3-dicarbonitrile. *J. Mol. Struct.* **2019**, *1181*, 25-37.
[26] Uzun, S.; Demircioğlu, Z.; Taşdoğan, M.; Ağar, E. Quantum chemical and X-ray diffraction studies of (E)-3-(((3,4-dimethoxybenzyl)imino)methyl)benzene-1,2-diol. *J. Mol. Struct.* **2020**, *1206*, 127749.
[27] Kansız, S.; Qadir, A.; Dege, N.; Faizi, S.H. Two new copper (II) carboxylate complexes based on *N*,*N*,*N*',*N*'-tetramethylethyleneamine: Synthesis, crystal structures, spectral properties, DFT studies and Hirshfeld surface analysis. *J. Mol. Struct.* **2021**, *1230*, 129916.
[28] Güzel, E.; Demircioğlu, Z.; Çiçek, C.; Ağar, E. Experimental and theoretical approach: Local and global chemical activity, charge transfer method with DNA bases, spectroscopic, structural and electronic properties of (E)-2-(((4-fluorophenyl)imino)methyl)-4-methoxyphenol. *J. Mol. Struct.* **2020**, *1204*, 127451.
[29] Mulliken, R.S. Electronic Population Analysis on LCAO-MO Molecular Wave Functions. I. *J. Chem. Phys.* **1955**, *23*, 1833-1840.
[30] Natorajan, S.; Shanmugam, G.; Martin, S.A. Growth and characterization of a new semi organic NLO material: L-tyrosine hydrochloride. *Cryst. Res. Technol.* **2008**, *43*, 561-564.
[31] Ayers, P.W.; Parr, R.G. Variational Principles for Describing Chemical Reactions: The Fukui Function and Chemical Hardness Revisited. *J. Am. Chem. Soc.* **2000**, *122*, 2010-2018.
[32] Bradshaw, D.S.; Andrews, D.L.; Nonlinear, J. Quantum Channels in Nonlinear Optical Processes, *Opt. Phys. Matt.* **2009**, *18*, 285-299.
[33] Evecen, M.; Tanak, H.; Alaman Ağar A.; Meral, S.; Özdemir, N. Comparative structural, spectroscopic and nonlinear optical analysis of a Schiff base compound with experimental and theoretical methods (HF, B3LYP and WB97X-D). *Optik* **2021**, *228*, 166133.
[34] Alyar, H.; Kantarci, Z.; Bahat, M.; Kasap, E. Investigation of torsional barriers and nonlinear optical (NLO) properties of phenyltriazines. *J. Mol. Struct.* **2007**, *834-836*, 516-520.
[35] Gansan Govindarajan, K.; Periandy, S.; Mohan, S. DFT (LSDA, B3LYP and B3PW91) comparative vibrational spectroscopic analysis of α-acetonaphthone. *Spectrochim. Acta A*. **2010**, *76*, 12.
[36] Demir, S.; Dincer, M.; Cukurovali, A.; Yilmaz, İ. Synthesis, characterization, and theoretical studies on *N'*-furan-2ylmethylene-*N*-[4-(3-methyl-3-phenyl-cyclobutyl)-thiazol-2-yl]-chloro-acetic acid hydrazide. *Mol. Cryst. Liq. Cryst.* **2016**, 629, *1*, 44-60.